DE GRUYTER High Temperature Materials and Processes 2022; 41: 296–305

Research Article

Kui-song Zhu, Xiang-kui Cheng, Yin-he Lin*, Ying-tao Zhao, Guo-liang Yin, Jing-wei Li*,
Jun Wang, and Li Cao

Pre-reduction of carbon-containing pellets of high chromium vanadium–titanium magnetite at different temperatures

https://doi.org/10.1515/htmp-2022-0006
received December 09, 2021; accepted December 27, 2021

Abstract: The effect of temperature on phase transformation, metallization rate, carbon residue and agglomeration of metal Fe after the pre-reduction of carbon-containing pellets in high-chromium vanadium–titanium magnetite (HCVTM) was investigated. The results indicated that titanomagnetite was finally reduced to metal Fe and (Mg, Fe) Ti_2O_5 without low valence titanium oxide with increasing pre-reduction temperature from 950 to 1,250°C; Vanadium magnetite produces Fe, VO and $VC_{0.88}$ without V, and chromite magnetite produces Fe, Cr_2O_3, CrC_x and a small amount of Cr. With an increase in the pre-reduction temperature, the metallization rate in the metallized pellets gradually increases, while the content of the residual carbon gradually decreases. Meanwhile, the iron particles precipitated on the surface of ore particles begin to soften into strips and finally agglomerate to form spherical iron particles, which leads to the diameter of iron particles increasing from 8.23 to 182.35 μm. When the pre-reduction temperature is 1,250°C, the maximum metallization rate in the metallized pellets is 92.49 wt% and the minimum content of residual carbon is 10.37 wt%.

Keywords: pre-reduction, carbon-containing pellets, high chromium vanadium–titanium magnetite, metallization rate, residual carbon

1 Introduction

Vanadium–titanium magnetite (VTM) is a kind of composite ore with the coexistence of iron, vanadium, titanium and other valuable elements. The VTM resources in China are mainly distributed in Panxi and Chengde, which reserves above 18 billion tons. Hongge mining area in Panzhihua has 3.6 billion tons of high-chromium vanadium–titanium magnetite (HCVTM) [1–3]. Due to the valuable chromium resources associated with this mineral, it has a higher comprehensive utilization value. At present, the smelting methods of VTM mainly include the blast furnace method and the non-blast furnace method. However, compared with ordinary VTM, the mineral composition of HCVTM is more complex, and the main phases of HCVTM are magnetite (Fe_3O_4), ilmenite ($FeTiO_3$), chromium magnetite ($FeCr_2O_4$), titanium magnetite ($Fe_{2.75}Ti_{0.25}O_4$) and vanadium magnetite (FeV_2O_4) [4]. The blast furnace smelting of HCVTM is the main method for recovering Fe and V. However, in the process of blast furnace smelting, the tailings discharge in the beneficiation process will be accompanied by the loss of vanadium and the titanium-containing phase grains in the slag after blast furnace smelting are fine and dispersed, resulting in a low comprehensive utilization rate of titanium recovered from high-titanium blast furnace slag [5,6], which makes it more difficult to blast-furnace smelting and comprehensive utilization of vanadium, titanium and chromium resources. Meanwhile, the chromium element with high content in the HCVTM enters the liquid iron with vanadium in the blast furnace smelting process and is oxidized into the vanadium slag after converting.

*** Corresponding author: Yin-he Lin,** School of Materials and Chemical Engineering, Yibin University, Yibin 644007, China, e-mail: linyinhe2009@163.com

*** Corresponding author: Jing-wei Li,** School of Materials Science and Engineering, Hefei University of Technology, Hefei 230009, China; Engineering Research Center of High Performance Copper Alloy Materials and Processing, Ministry of Education, Hefei 230009, China; State Key Laboratory of Mineral Processing, BGRIMM Technology Group, Beijing 100160, China; State Key Laboratory of Complex Nonferrous Metal Resources Clean Utilization, Kunming University of Science and Technology, Kunming 650504, China, e-mail: jwli@hfut.edu.cn

Kui-song Zhu, Xiang-kui Cheng, Ying-tao Zhao, Jun Wang, Li Cao: School of Vanadium and Titanium, Panzhihua University, Panzhihua 617000, Sichuan, China

Guo-liang Yin: School of Materials and Chemical Engineering, Yibin University, Yibin 644007, China

Therefore, the chromium element has not been recovered and utilized, and other rare metal elements such as cobalt, nickel, scandium and gallium have not been utilized and also enter into the slag. Therefore, the blast furnace smelting process of HCVTM reduces the recovery and utilization of Fe, V, Ti and Cr in the mineral. It is particularly important to develop the non-blast furnace smelting technology of HCVTM.

At present, the typical non-blast furnace smelting process of HCVTM is the pre-reduction of HCVTM to prepare metallized pellets, then the preparation of the Fe–V–Cr alloy and titanium-containing slag by electric furnace melting of metallized pellets. Li et al. [7] carried out an oxidation roasting gas-based direct reduction experiment with HCVTM; the result shows that pellets with different metallization rates are melted and separated in an electric furnace to obtain the titanium-containing slag and Fe–V–Cr alloy. The TiO_2 grade in the titanium-containing slag was 39.36 wt%, and the yield was 89.69%. The TFe content in the Fe–V–Cr alloy was 92.34 wt%, and the yield of Fe, V, Cr was 93.53, 85.68, and 89.50%, respectively. He et al. [8] used HCVTM-containing TFe: (52.29 wt%), Cr_2O_3 (0.48 wt%) and Fe_2O_3 (27.25 wt%) for direct reduction-furnace smelting experiment, and the migration law of iron, vanadium and titanium during the smelting process were analysed by thermodynamic calculation at different C and O molar ratios. The results show that the recovery rate of Fe, V and Ti increases with an increase in n_C/n_O and melting temperature, respectively. When the n_c/n_o ratio is greater than 1.15, the recovery rate of Fe, V and Ti reaches 90%. The suitable optimum conditions for melting separation of metal and slag are temperature $T = 1,678$ K and $n_C/n_O = 1.16$. Zhou et al. [9] carried out a direct reduction of HCVTM based on thermodynamic calculation. The results show that the minimum reduction temperature of HCVTM is 860°C, but the reduction of Cr is difficult to achieve at this temperature, and the minimum reduction temperature of V is above 700°C. When the temperature is 1,350°C, C/O is 1.0, and the reduction time is 30 min, HCVTM can be completely reduced, and the reduction degree can reach 0.98. When C/O was lower than 1.0, $FeTi_2O_5$ was the reduction intermediate product of $FeO{\cdot}TiO_2$. When C/O was 1.0, HCVTM can be completely reduced to Fe and TiO_2. Therefore, in the direct reduction-melting process of HCVTM, there are multiple ways to recover Fe, V, Ti and Cr, which can further improve the metal recovery rate and utilization rate. However, according to the analysis of the current research status of pre-reduction, there are few studies on the metallization rate and the residual carbon content in the metal pellets after the pre-reduction of HCVTM. Metallization rate and the residual carbon content in the metal pellets can determine the final reduction degree of residual oxides in the metallized pellets and the selection of melting and separation temperature of metal and slag in the subsequent electric furnace melting process, which are the key factors to improve the direct reduction-melting separation of HCVTM, recover valuable metals and prepare titanium-rich slag.

Hence, HCVTM in the Hongge mining area of Panxi area was selected as raw material combined with the HCVTM pre-reduction-electric furnace melting separation process. The pre-reduction experiment of carbon distribution pellets in HCVTM was investigated. The effects of the pre-reduction temperature on the metallization rate and residual carbon of pellets after pre-reduction are mainly studied, which lays a foundation for the selection of final reduction and melting separation process parameters of subsequent metallized pellets.

2 Experimental

2.1 Materials

The main raw materials for the preparation of HCVTM carbon-containing pellets are HCVTM in the Hongge mining area, PVA (polyvinyl alcohol) and anthracite powder. The chemical compositions of HCVTM and anthracite powder are listed in Tables 1 and 2. The phase characteristics of HCVTM were investigated using X-ray diffraction (XRD) with the obtained results shown in Figure 1.

As shown in Figure 1, the main Fe-bearing phases in HCVTM are magnetite (Fe_3O_4), chromite magnetite ($FeCr_2O_4$), titanomagnetite ($Fe_{2.75}Ti_{0.25}O_4$), ilmenite ($FeTiO_3$) and vanadium magnetite (FeV_2O_4). TiO_2 is mainly enriched in titanomagnetite and a small amount of ilmenite, V_2O_5 is mainly

Table 1: Chemical compositions of HCVTM (wt%)

TFe	FeO	TiO_2	SiO_2	Al_2O_3	MgO	CaO	V_2O_5	Cr_2O_3	P	S
50.16	26.47	12.44	4.60	2.58	3.68	0.48	0.57	1.28	<0.01	0.15

Table 2: Chemical compositions of anthracite powder (wt%)

Fixed carbon	Moisture	Ash	Volatile
78.03	9.5	10.5	1.1

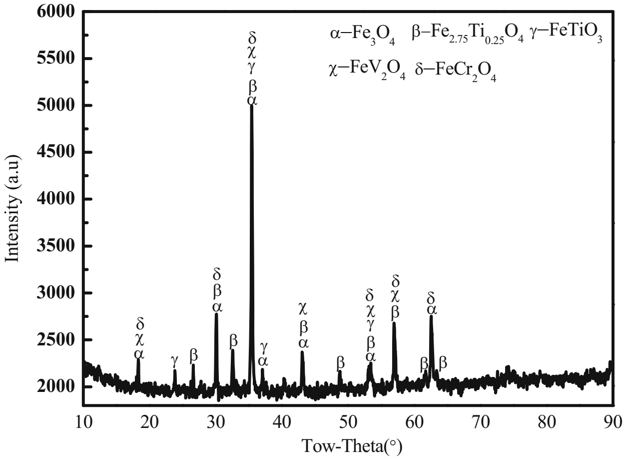

Figure 1: X-ray diffraction analysis of HCVTM.

enriched in vanadium magnetite and Cr_2O_3 is mainly enriched in chromite magnetite.

2.2 Experimental procedure

The pre-reduction experiment of HCVTM was carried out at 950, 1,000, 1,050, 1,100, 1,150, 1,200, and 1,250°C for 30 min by using HCVTM pellets with C and O molar ratio (n_C/n_O) of 1.5 as raw materials. The pellets with $n_C/n_O = 1.5$ were placed in a corundum crucible with an inner diameter of 50 mm, an outer diameter of 55 mm and a height of 150 mm, respectively. Each carbon-containing pellet is about 25 mm in diameter and 15 mm in thickness. Then, the corundum crucible was placed in a high-temperature box-type resistance furnace, and the pre-reduction temperatures were 950, 1,000, 1,050, 1,100, 1,150, 1,200, and 1,250°C; the pre-reduction time was 30 min. After pre-reduction, the metallized pellets were taken out, then the pulverized coal was used to cover them. Metallized pellets are covered with anthracite powder until the temperature of metallized pellets cools to the room temperature. Subsequently, the metallized pellets were removed and ground by a ball mill. The phase in the metallized pellets after pre-reduction was detected by XRD analysis. The contents of TFe, MFe and C in pellets were measured by chemical analyses. The metallized pellets were cut along the longitudinal by a diamond wire cutting machine. After polishing, the microstructures of the different enrichment layers were observed using a scanning electron microscope (SEM).

In the experiment, the calculation of the molar ratio of carbon to oxygen (n_C/n_O) and metallization rate of metallized pellets is shown in equations (1) and (2), respectively.

$$n_C/n_O = \frac{m_C/M_C}{m_O/M_O}\frac{\frac{m_{AD}\times w_C}{M_C}}{\frac{m_{HCVTM}\times w_O}{M_O}} = \frac{\frac{m_{AD}\times w_C}{M_C}}{\frac{m_{HCVTM}\times (w_{O,Fe_2O_3}+w_{O,FeO})}{M_O}}, \tag{1}$$

m_{AD} is the mass of anthracite powder, g; m_{HCVTM} is the mass of HCVTM, g; w_C is the mass fraction of fixed carbon in anthracite, wt%; w_O is the mass fraction of oxygen in HCVTM, wt%; W_{O,Fe_2O_3} is the mass fraction of oxygen in Fe_2O_3, wt%; $w_{O,FeO}$ is the mass fraction of oxygen in FeO, wt%; M_C is the molar mass of carbon, g·mol^{-1} and M_O is the molar mass of oxygen, g·mol^{-1}.

$$\eta = \frac{M_{Fe}}{T_{Fe}} \times 100\%, \tag{2}$$

η is the metallization rate, %; M_{Fe} is the mass fraction of metallic iron in reduced samples, wt% and T_{Fe} is the mass fraction of total iron in reduced samples, wt%.

3 Results and discussion

3.1 Effect of pre-reduction temperature on phase transformation of HCVTM

The main phases of metallized pellets obtained by HCVTM pellets with carbon at different pre-reduction temperatures for 30 min are shown in Figure 2. Table 3 lists the possible chemical reaction equations of titanomagnetite in the reduction process of HCVTM and the relationship between Gibbs free energy and temperature [10,11].

According to the results of the previous studies on the composition of HCVTM, titanomagnetite in VTM is a solid solution composed of magnetite (Fe_3O_4) and ulvspinel (Fe_2TiO_4). The expression of this solid solution is $xFe_3O_4{\cdot}yFe_2TiO_4$. According to the different solid solution degrees of magnetite (Fe_3O_4) and ulvspinel (Fe_2TiO_4), the chemical formula of titanomagnetite can be expressed as $Fe_{2.75}Ti_{0.25}O_4$, $Fe_{2.5}Ti_{0.5}O_4$ and $Fe_{2.25}Ti_{0.75}O_4$, which are composed of $3Fe_3O_4{\cdot}Fe_2TiO_4$, $Fe_3O_4{\cdot}Fe_2TiO_4$ and $Fe_3O_4{\cdot}3Fe_2TiO_4$, respectively. Therefore, when the carbon-containing pellets of HCVTM are pre-reduced at different temperatures, according to equations (3)–(6) given in Table 3, it can be

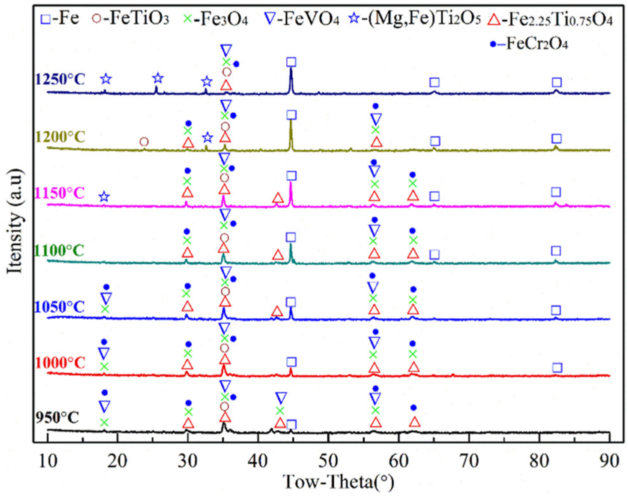

Figure 2: XRD patterns of metallized pellets after reduction at different pre-reduction temperatures.

seen that Fe_3O_4 in the titanium magnetite composed of HCVTM will be reduced to FeO at 681°C. Then, the FeO begins to be reduced to metallic Fe at 719°C. Therefore, during the pre-reduction process of HCVTM, the Fe_3O_4 that forms titanium magnetite will be continuously reduced to FeO and Fe, so that the content of Fe_3O_4 dissolved in titanium magnetite will gradually decrease, leading to the gradual reduction of titanium magnetite to ulvspinel (Fe_2TiO_4) and Fe.

However, according to Figure 2, there is no ulvspinel (Fe_2TiO_4) in the metallized pellets after pre-reduction at 950–1,250°C. According to equation (8) given in Table 3, ulvspinel (Fe_2TiO_4) is unstable and will begin to be reduced to ilmenite ($FeTiO_3$) by CO at 427°C. Therefore, $FeTiO_3$ can be found in XRD results at different temperatures. It can be considered that ulvspinel (Fe_2TiO_4) exists in the form of $FeTiO_3$ in the reduction process. However, there are two paths in the reduction process of ilmenite ($FeTiO_3$): (1) If the pre-reduction temperature is between 67 and 1,010°C, the ilmenite will occur, equation (11) and (12) in Table 3, and then the ilmenite ($FeTiO_3$) will be reduced to Fe and low valence titanium oxides; (2) if the temperature is higher than 1,010°C, the ilmenite will undergo equation (9) given in Table 3 and the ilmenite ($FeTiO_3$) will be reduced to metallic Fe and $FeTi_2O_5$ (pseudobrookite) by CO. Moreover, $FeTi_2O_5$ (pseudobrookite) will participate in equation (10) given in Table 3 and continue to be reduced to Fe and low valence titanium oxides by CO. However, combined with Figure 2, TiO_2 and the other low valence titanium oxides do not appear in the temperature range of 950–1,250°C, (Mg, Fe)Ti_2O_5 begins to appear in metallized pellets at 1,200°C. Some studies [12–14] investigated that the atomic radius of Mg^{2+} and Fe^{2+} are relatively close; thus, Mg^{2+} can easily replace the position of Fe^{2+} in $FeTi_2O_5$ (pseudobrookite) to form magnesium-containing pseudobrookite. Thus, (Mg, Fe) Ti_2O_5 appears in the XRD pattern of metallized pellets after pre-reduction at 1,200°C. In the pre-reduction process, ilmenite should be pre-reduced according to the high-temperature reduction route and produce Fe and $FeTi_2O_5$ (pseudobrookite). As the temperature rises to 1,250°C, the number of diffraction peaks of (Mg, Fe) Ti_2O_5 phase increases, while the number of diffraction peaks of ilmenite ($FeTiO_3$) phase decreases obviously. For this reason, ilmenite ($FeTiO_3$) is greatly reduced to $FeTi_2O_5$ (pseudobrookite) at 1,250°C, increasing the number of diffraction peaks of $FeTi_2O_5$ (pseudobrookite). The Mg^{2+} replaces the position of Fe^{2+} in $FeTi_2O_5$ (pseudobrookite) to form magnesium-containing pseudobrookite. According to the thermodynamic calculation results, ilmenite ($FeTiO_3$) will be reduced to Fe and $FeTi_2O_5$ (pseudobrookite) by CO at 1,010°C, but the (Mg, Fe) Ti_2O_5 phase appears in the XRD pattern at 1,200°C, and the content of (Mg, Fe)Ti_2O_5 phase

Table 3: Possible chemical reactions of titanium magnetite and magnetite in HCVTM [10,11]

No.	Chemical equation	$\Delta G^\theta – T$	Reduction temperature (°C)
3	$Fe_3O_4 + C = 3FeO + CO(g)$	$\Delta G^\theta = 207{,}510 - 217.62T$	681
4	$FeO + C = Fe + CO(g)$	$\Delta G^\theta = 158{,}970 - 160.25T$	719
5	$Fe_3O_4 + CO = 3FeO + CO_2(g)$	$\Delta G^\theta = 35{,}380 - 40.16T$	608
6	$FeO + CO = Fe + CO_2(g)$	$\Delta G^\theta = -13{,}160 + 17.21T$	765
7	$Fe_2TiO_5 + CO = Fe_2TiO_4 + CO_2$	$\Delta G^\theta = -9{,}785 - 4.95T$	−1,704
8	$Fe_2TiO_4 + CO = FeTiO_3 + Fe + CO_2$	$\Delta G^\theta = -4{,}550 + 6.5T$	427
9	$2FeTiO_3 + CO = FeTi_2O_5 + Fe + CO_2$	$\Delta G^\theta = 10.1 - 0.01T$	1,010
10	$3FeTi_2O_5 + 5CO = 2Ti_3O_5 + 3Fe + 5CO_2$	$\Delta G^\theta = 20.65 - 0.0371T$	557
11	$3/4FeTiO_3 + C = 3/4Fe + 1/4Ti_3O_5 + CO$	$\Delta G^\theta = 184.07 - 0.2742T$	671
12	$2/3FeTiO_3 + C = 2/3Fe + 1/3Ti_2O_3 + CO$	$\Delta G^\theta = 213{,}000 - 171.00T$	972
13	$2Fe_2TiO_4 + MgO + 4CO = MgTi_2O_5 + 4Fe + 4CO_2$	$\Delta G^\theta = 637.45 - 0.605T$	781

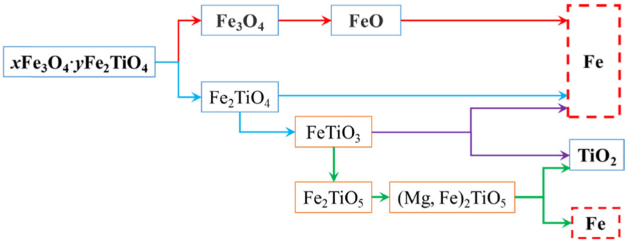

Figure 3: Reduction paths of titanomagnetite in HCVTM.

increases significantly at 1,250°C. Therefore, it can be inferred that when the pre-reduction temperature is about 1,200°C, ilmenite ($FeTiO_3$) in HCVTM will be reduced to Fe and $FeTi_2O_5$ (pseudobrookite) by CO, and the reaction rate will be accelerated at 1,250°C.

Hence, the reduction paths of titanomagnetite in HCVTM during pre-reduction can be summarized as shown in Figure 3.

During the pre-reduction of HCVTM, the possible reactions of vanadium magnetite and chromium magnetite are given in Tables 4 [15] and 5 [16,17]. The Gibbs free energy of reaction equation given in Tables 4 and 5 is calculated, and the calculation results are shown in Figure 4.

In this work, the pre-reduction temperature range is in the range of 950–1,250°C. According to the thermodynamic calculation results given in Table 4, when the pre-reduction temperature is 848°C, FeO in vanadium magnetite $FeO{\cdot}V_2O_3$ (FeV_2O_4) begins to be reduced to Fe as equation (14) given in Table 4, resulting in the gradual reduction of FeO content in solid solution to vanadium magnetite, and vanadium magnetite will eventually change to V_2O_3. When the temperature rises to 1,021°C, the vanadium magnetite undergoes equation (15), and V_2O_3 in vanadium magnetite begins to be reduced to VO; when the temperature is 1,025°C, the equation (17) may occur and start to generate $VC_{0.88}$. It can be seen from equation (16) that metal V cannot be generated under the whole pre-reduction temperature range. According to Figure 4(a), when the pre-reduction temperature is 950 and 1,000°C, V in the metallized pellets may exist in the form of vanadium magnetite (FeV_2O_4) and V_2O_3. Meanwhile, XRD results also show that there is a diffraction peak of vanadium magnetite $FeO{\cdot}V_2O_3$ (FeV_2O_4) at 950 and 1,000°C, as shown in Figure 2, but no diffraction peak of V_2O_3 is found in Figure 2, which may be mainly due to the low content of V in the raw ore, Measured by V_2O_5, the mass fraction is only 0.57 wt%, as given in Table 1; thus, it is lower than the lowest limit of XRD detection; thus, no diffraction peak of V_2O_3 is found in Figure 2. As the pre-reduction temperature increases to 1,050°C, the possible V-containing phases in the metallized pellets are vanadium magnetite $FeO{\cdot}V_2O_3$ (FeV_2O_4), VO, V_2O_3 and $VC_{0.88}$. But according to Figure 4(a), it can be found that when the temperature is larger than 1,000°C, the ΔG^{θ}-T position of equation (17) is lower than that of equation (15), thus the possibility of occurrence of equation (17) is larger than that of equation (15). Therefore, when the pre-reduction temperature is larger than 1,050°C, the V-containing phases in the metallized pellets may be vanadium magnetite $FeO{\cdot}V_2O_3$ (FeV_2O_4), VO and $VC_{0.88}$.

When the pre-reduction experiment of chromite magnetite is carried out at 950–1,250°C, according to the thermodynamic calculation results given in Table 5, when the temperature is higher than 994°C, FeO in chromite begins to be reduced to metallic Fe, resulting in the gradual reduction of FeO content in chromite $FeCr_2O_4$. Meanwhile, when the temperature is higher than 1,200°C, chromite $FeCr_2O_4$ ($FeO{\cdot}Cr_2O_3$) begins to be reduced to Cr by equation (19) given in Table 5. Therefore, when the pre-reduction temperature is lower than 1,100°C, the possible phases in the metallized pellets are chrome magnetite $FeCr_2O_4$ ($FeO{\cdot}Cr_2O_3$) and Cr_2O_3; according to equations (20) and (21) given in Table 5, CrC_x ($0 < x < 1$) may be generated in the metallized pellet at 1,150°C. Meanwhile, as shown in Figure 4(b), the $\Delta G^{\theta}-T$ position of equation (18) is the lowest at this temperature condition. Thus, equations (18) is the most likely to occur at 1,150°C. Then, the main reaction of chromite magnetite is that $FeCr_2O_4$ ($FeO{\cdot}Cr_2O_3$) is reduced to Cr_2O_3. When the temperature is larger than 1,200°C, the thermodynamic calculation results show that metal Cr may be generated. However, according to Figure 4(b), the ΔG^{θ}-T position of equation (19) is the highest than others; thus, this reaction is difficult to occur. But there may be a small amount of metal Cr in the metallized pellets. Therefore, when the

Table 4: Possible chemical reactions of vanadium magnetite in HCVTM [15]

No.	Chemical equation	$\Delta G^{\theta}-T$	Reduction temperature (°C)
14	$FeO{\cdot}V_2O_3 + CO = V_2O_3 + Fe + CO_2$	$\Delta G^{\theta} = 164.84 - 0.147T$	848
15	$FeO{\cdot}V_2O_3 + 2CO = 2VO + Fe + 2CO_2$	$\Delta G^{\theta} = 399.74 - 0.309T$	1,021
16	$FeO{\cdot}V_2O_3 + 4CO = 2V + Fe + 4CO_2$	$\Delta G^{\theta} = 1003.88 - 0.63T$	1,320
17	$FeO{\cdot}V_2O_3 + 7.52CO = 2VC_{0.88} + Fe + 5.76CO_2$	$\Delta G^{\theta} = 806.13 - 0.621T$	1,025

Table 5: Possible chemical reactions of chromium magnetite in HCVTM [16,17]

No.	Chemical equation	ΔG^{θ}–T	Reduction temperature (°C)
18	$FeCr_2O_4 + CO = Fe + Cr_2O_3 + CO_2(g)$	$\Delta G^{\theta} = 205.23 - 0.162T$	994
19	$FeCr_2O_4 + 4CO = Fe + 2Cr + 4CO_2(g)$	$\Delta G^{\theta} = 975.03 - 0.662T$	1,200
20	$7FeCr_2O_4 + 40CO = 7Fe + 2Cr_7C_3 + 34CO_2(g)$	$\Delta G^{\theta} = 652.18 - 0.471T$	1,133
21	$2/3Cr_2O_3 + 54/23C = 4/69Cr_{23}C_6 + 2CO(g)$	$\Delta G^{\theta} = 494.37 - 0.342T$	1,112

temperature is 1,200–1,250°C, the possible Cr-containing phases in the metallized pellets are $FeCr_2O_4$ ($FeO{\cdot}Cr_2O_3$), Cr_2O_3, CrC_x and Cr.

Therefore, according to the thermodynamic calculation results and the phase analysis results of metallized pellets at different pre-reduction temperatures, it can be seen that with the increase in pre-reduction temperature, the metallization rate of pre-reduced pellets should increase, and the metallization rate obtained by pre-reduction at 1,250°C is the largest. However, the pre-reduction degree of the metallized pellets obtained by pre-reduction at 1,250°C is not complete. There may be a small amount of (Mg, Fe) Ti_2O_5, $FeO{\cdot}V_2O_3$ (FeV_2O_4) and $FeCr_2O_4$ ($FeO{\cdot}Cr_2O_3$) in the metallized pellets, which cannot be completely reduced to metallic Fe. Meanwhile, the vanadium magnetite $FeO{\cdot}V_2O_3$ (FeV_2O_4) cannot be reduced to metallic V but exists in the form of vanadium magnetite $FeO{\cdot}V_2O_3$ (FeV_2O_4), VO and $VC_{0.88}$ in the metallized pellets. A small amount of chromite magnetite $FeCr_2O_4$ ($FeO{\cdot}Cr_2O_3$) may be reduced to metallic Cr, while other chromite magnetite $FeCr_2O_4$ ($FeO{\cdot}Cr_2O_3$) after pre-reduction exists in metallized pellets in the form of $FeCr_2O_4$ ($FeO{\cdot}Cr_2O_3$), Cr_2O_3 and CrC_x. Therefore, when the pre-reduction temperature is 950–1,250°C, the pre-reduction of HCVTM can only be carried out to reduce Fe in titanomagnetite, chromium magnetite and vanadium magnetite. While the reduction of V and Cr, especially the reduction of metal V, which will not occur in the pre-reduction process, and a small amount of chromium magnetite $FeCr_2O_4$ ($FeO{\cdot}Cr_2O_3$) may be reduced to metallic Cr. Therefore, the deep reduction of vanadium magnetite and chromite magnetite to obtain V and Cr depends on the high temperature provided by the subsequent furnace melting process.

3.2 Effect of pre-reduction temperature on metallization rate and residual carbon in metallized pellets

The metallization rate and carbon residue in the metallized pellets obtained after pre-reduction at the temperature of 950–1,250°C are shown in Figure 5.

As shown in Figure 5, when the pre-reduction temperature increases from 950 to 1,250°C, the metallization rate in the metallized pellets gradually increases from 27.97 to 92.49 wt%. However, it can be found from Figure 5 that the increasing trend of metallization rate in metallized pellets exhibits two states: when the temperature is lower than 1,050°C, the metallization rate increases slowly and the metallization rate of metallized pellets is small; when the

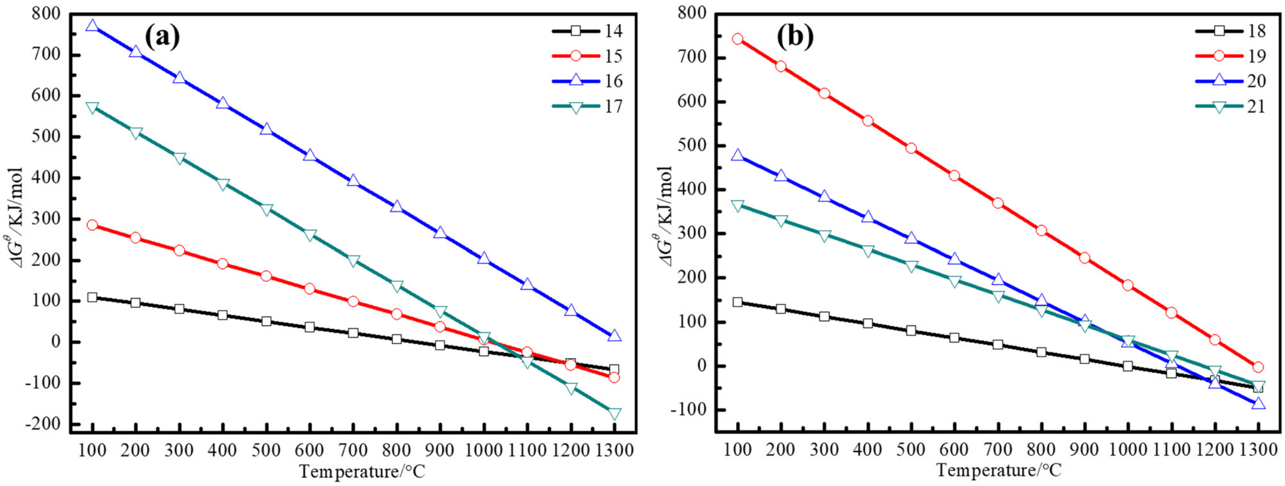

Figure 4: ΔG^{θ}–T diagram of possible chemical reaction equations during pre-reduction of vanadium magnetite and chrome magnetite: (a) vanadium magnetite, (b) chrome magnetite.

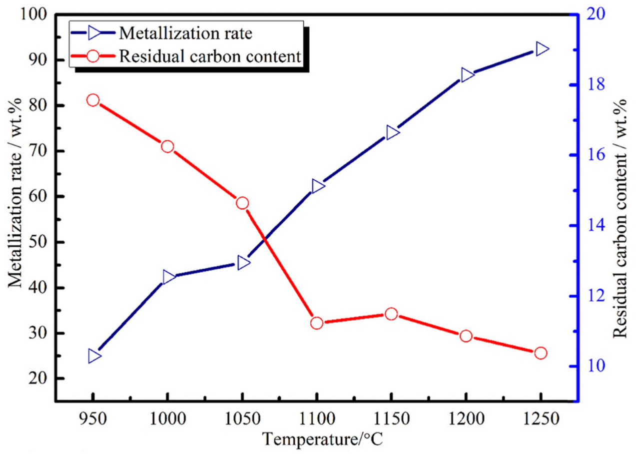

Figure 5: Metallization rate and carbon residue in metallized pellets were obtained at different pre-reduction temperatures.

temperature was higher than 1,050°C, the metallization rate of the pre-reduced pellets showed a sharp increase. Combined with the thermodynamic analysis results, it can be indicated that when the temperature is higher than 681°C, magnetite begins to be reduced to metallic Fe, as shown in equation (3) given in Table 3, but this reaction is a solid reduction process of magnetite; thus, the chemical reaction rate is slow. Thus, when the temperature is lower than 1,050°C, Fe_3O_4 in HCVTM is mainly reduced, while the gasification reaction of C in the pellets is weak in this temperature range, resulting in a lower partial pressure of CO. Therefore, the reduction degree of titanium magnetite, vanadium magnetite and chromium magnetite is lower, resulting in a lower metallization rate of the pellets. Meanwhile, as shown in Figure 5, at the range of 950–1,050°C, the amount of residual carbon in metallized pellets also decreases slowly with the increase of temperature, which can indirectly explain the gasification reaction rate of C in this temperature range is low. When the temperature range is 1,050–1,100°C, as shown in Figure 5, the residual carbon in metallized pellets decreases sharply with increasing temperature. Therefore, within this temperature range, the gasification reaction rate of C is the largest, and the partial pressure of CO in the furnace increases. Therefore, after 1,100°C, titanomagnetite, vanadium magnetite and chromium magnetite in HCVMT participate in the reduction. As a result, the metallization rate in the metallized pellet will continue to increase. When the temperature increases to 1,250°C, the maximum metallization rate in the metallized pellet is 92.49 wt%. And, the content of residual C in the pellet is 10.37 wt%. Therefore, residual C can be used as the reducing agent for a deep reduction in the subsequent electric furnace melting and separation process to further reduce HCVMT.

3.3 Effect of pre-reduction temperature on Fe agglomeration in metallized pellets

The microstructures of the metallized pellets obtained by pre-reduction of HCVTM at 950–1,250°C are shown in Figure 6. Figure 6(a) is the microstructure of HCVTM raw ore, Figure 6(b)–(h) is the microstructure morphology of metallized pellets after pre-reduction at 950–1,250°C and Figure 6(i) is the microstructure of the cross-section of the metallized pellets after pre-reduction at 1,250°C.

As shown in Figure 6, magnetite, titanomagnetite, chrome magnetite and vanadium magnetite of HCVTM form irregular block structures in the form of symbiosis and association. When the pre-reduction temperature was 950°C, the block structure showed that it became loose and porous, and no iron particles or iron beads were observed. When the pre-reduction temperature is 1,000°C, the microstructure shows that the surface of the ore particles in the form of a loose porous structure, and compared with the block structure at 950°C, the surface of the block structure became loose and porous; however, no iron particles or iron beads were observed on the surface of mineral particles. When the pre-reduction temperature is 1,000°C, the microstructure shows that the surface of the massive ore particles presents a loose porous structure. Compared with the massive structure at 950°C, the massive structure splits at 1,000°C and then becomes a smaller massive structure, as shown in Figure 6(c). When the pre-reduction temperature was 1,050°C, the microstructure showed that iron beads began to appear on the surface of loose and porous ore particles. However, the average particle size of iron beads was about 8.23 µm measured by the SEM. Meanwhile, iron beads were also found only in the local area of the ore particle surface as shown in Figure 6(d). When the pre-reduction temperature increased to 1,100°C, as shown in Figure 6(e), the number of iron beads on the surface of the ore particles was significantly more than that of the sample after pre-reduction at 1,050°C. The average particle size of the iron beads was about 24.26 µm. When the pre-reduction temperature was 1,150°C, as shown in Figure 6(f), and the microstructure on the surface of the ore particles showed that the number of iron beads increased significantly. After the iron beads were precipitated on the surface of the ore particles, the shrinkage phenomenon appeared. Moreover, the iron beads on the surface of the local ore particles have been agglomerated, and the particle size of the iron beads has increased obviously. The average particle size of the iron beads is about 56.58 µm at 1,150°C. When the pre-reduction temperature was 1,200°C, which can be found in Figure 6(g) that the precipitated iron beads had an

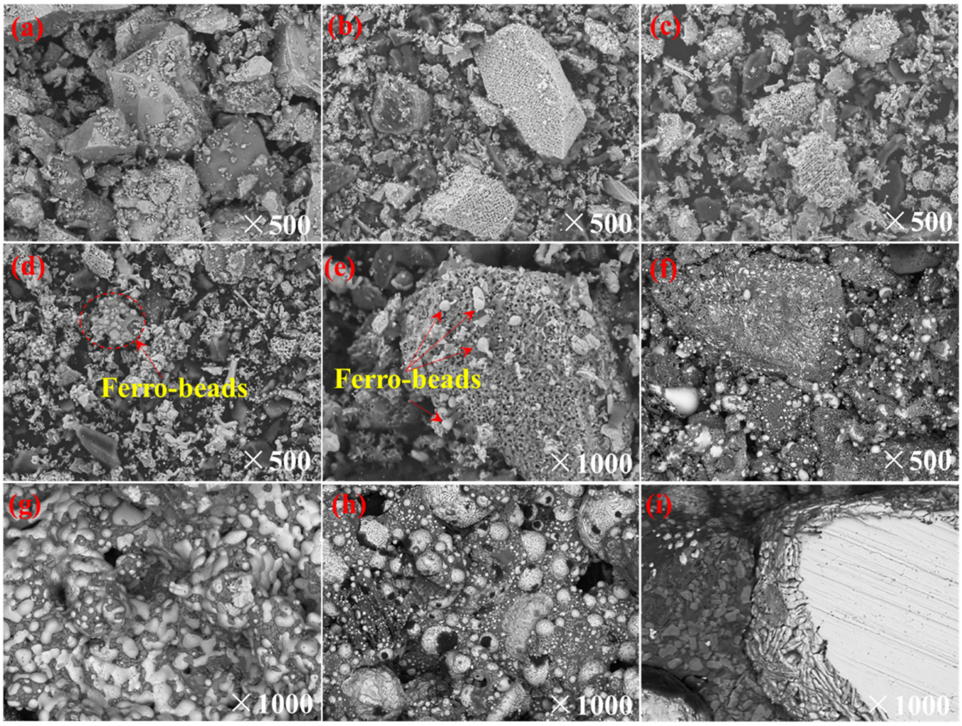

Figure 6: Microstructures of metallized pellets after different pre-reduction temperatures of high-chromium vanadium–titanium magnetite: (a) raw ore, (b)–(h) pre-reduction temperature 950–1,250°C and (i) microstructure of cross-section of metallized pellets at a pre-reduction temperature of 1,250°C.

obvious softening phenomenon, then gradually changed from the previous spherical shape to the strip-shaped iron particles; while the strip-shaped iron particles wrapped the ore particles. When the temperature rises to 1,250°C, the softened iron particles begin to agglomerate and form spherical iron particles as shown in Figure 6(h). The average diameter of the spherical iron particles is about 182.35 μm. Moreover, it can be found from Figure 6(i) that there is still the agglomeration morphology of strip iron particles on the surface of spherical iron particles with large particles, indicating that the strip iron particles are interconnected to form spherical iron particles with large particles after softening. And, there is no slag phase after softening the iron particles.

Therefore, according to the results of the microstructures of metal pellets after pre-reduction, it can be found that the ore particles gradually change from block structure to loose and porous surface at a pre-reduction temperature of 950–1,000°C, and the large ore particles gradually crack into small block structure, which can significantly improve the dynamic conditions of pre-reduction, but no iron beads are precipitated on the surface of ore particles. When the temperature rises to 1,050°C, iron beads begin to precipitate on the surface of ore particles. When the temperature rises to 1,150°C, the number of iron beads on the surface of ore particles increases significantly, and the particle size of iron beads becomes larger. When it reaches 1,200°C, the iron beads begin to soften and hook up to form strip iron particles. When the temperature is 1,250°C, the strip iron particles hook up and accumulate to form spherical iron particles, and the average particle size of spherical iron particles is 182.35 μm. Therefore, in the pre-reduction process of HCVTM, when the pre-reduction temperature is higher than 1,000°C, iron beads begin to precipitate on the surface of ore particles. With the increase in temperature, spherical iron beads change into strip iron particles at about 1,200°C. At 1,250°C, strip iron particles agglomerate and turn into spherical iron beads, so increasing the temperature is conducive to improving the enrichment and agglomeration of metallic iron.

4 Conclusion

The pre-reduction of HCVTM with carbon pellets was carried out at the range of 950–1,250°C. The phase transformation law of HCVTM, metallization rate, and the precipitation and agglomeration of the Fe phase in metallized pellets at different pre-reduction temperatures were analysed.

1. At the pre-reduction temperature range of 950–1,250°C, titanomagnetite in HCVTM is finally reduced to metal Fe and (Mg, Fe)Ti_2O_5, and low valence titanium oxide will not appear. Vanadium magnetite produces Fe, VO, and $VC_{0.88}$ without metal V; chromite magnetite produces Fe, Cr_2O_3, CrC_x and a small amount of metal Cr.
2. With an increase in the pre-reduction temperature, the metallization rate in the metallized pellets obtained after pre-reduction of HCVTM gradually increases, while the content of residual carbon gradually decreases. When the pre-reduction temperature is 1,250°C, the maximum metallization rate in the metallized pellets is 92.49 wt%, and the minimum content of residual carbon is 10.37 wt%.
3. With the increase of pre-reduction temperature, the bulk surface of HCVTM gradually becomes loose and porous; then. the large block structure gradually split into small particles. Meanwhile, the iron particles precipitated on the surface of ore particles begin to soften into strips with an increase in temperature and finally agglomerate to form spherical iron particles, which leads to a diameter of iron particles increases from 8.23 to 182.35 μm.

Acknowledgments: This research was supported by the Project of the National Natural Science Foundation of China (Grant No. U1960101, No. 51874272 and No. 52111540265), Sichuan Science and Technology Program (No. 2021 YJ0548), Chongqing Municipal Natural Science Foundation (cstc2020jcyj-msxmX0060), Panzhihua Science and Technology Project (Grant No. 2020CY-G-15), The Open Project of the State Key Laboratory of Advanced Metallurgy (KF20-03), Key Laboratory of Comprehensive Utilization of Vanadium and Titanium Resources in Sichuan Province (2019FTSZ06, 2020FTSZ01), the Ph.D. Fund of Panzhihua University, and funded by the State Key Laboratory of Vanadium and Titanium Resources Comprehensive Utilization, Open Foundation of State Key Laboratory of Mineral Processing (No. BGRIMM-KJSKL-2022-23) and Open Foundation of State Key Laboratory of Complex Nonferrous Metal Resources Clean Utilization (No. CNMRCUKF2205).

Funding information: This research was supported by the Project of the National Natural Science Foundation of China (Grant No. U1960101, No. 51874272 and No. 52111540265), Sichuan Science and Technology Program (No. 2021YJ0548), Chongqing Municipal Natural Science Foundation (cstc2020jcyj-msxmX0060), Panzhihua Science and Technology Project (Grant No. 2020CY-G-15), The Open Project of the State Key Laboratory of Advanced Metallurgy (KF20-03), Key Laboratory of Comprehensive Utilization of Vanadium and Titanium Resources in Sichuan Province (2019FTSZ06), the Ph.D. Fund of Panzhihua University, and funded by the State Key Laboratory of Vanadium and Titanium Resources Comprehensive Utilization, Open Foundation of State Key Laboratory of Mineral Processing (No. BGRIMM-KJSKL-2022-23) and Open Foundation of State Key Laboratory of Complex Nonferrous Metal Resources Clean Utilization (No. CNMRCUKF2205).

Author contributions: Kui-song Zhu: experimental investigation, writing – original draft, analysis, writing – review & editing. Xiang-kui Cheng and Ying-tao Zhao: investigation, visualization, supervision, funding acquisition, formal analysis. Yin-he Lin: investigation, visualization, funding acquisition. Guo-liang Yin: investigation, visualization, funding acquisition. Jing-wei Li: investigation, visualization, funding acquisition. Li Cao: experimental investigation, writing – review & editing, drafting. Jun Wang: drafting, methodology, writing – review editing, validation.

Conflict of interest: Authors state no conflict of interest.

References

[1] Du, G. H. *Principle of blast furnace smelting vanadium titanium magnetite*. Science Press, Beijing, 1996.

[2] Peng, Y. J. and C. Lv. Mining. Comprehensive utilization status and progress of vanadium titano-magnetite. *Research for Development*, Vol. 226, 2019, pp. 134–139.

[3] Zhao, W., M. S. Chu, H. W. Guo, Z. G. Liu, and B. J. Yan. Softening–melting–dripping characteristics and evolution mechanism of vanadium-bearing titanomagnetite carbon composite briquette used as novel blast furnace burden. *Journal of Iron and Steel Research International*, Vol. 28, No. 9, 2021, pp. 1082–1094.

[4] Zhao, L. S., L. N. Wang, T. Qi, D. S. Chen, H. X. Zhao, and Y. H. Liu. A novel method to extract iron, titanium, vanadium, and chromium from high-chromium vanadium-bearing titanomagnetite concentrates. *Hydrometallurgy*, Vol. 149, 2014, pp. 106–109.

[5] Sun, H. Y., J. S. Wang, Y. H. Han, X. F. She, and Q. G. Xue. Reduction mechanism of titanomagnetite concentrate by hydrogen. *International Journal of Mineral Processing*, Vol. 125, 2013, pp. 122–128.

[6] Chen, S. Y. and M. S. Chu. Metalizing reduction and magnetic separation of vanadium titano-magnetite based on hot briquetting. *International Journal of Minerals Metallurgy and Materials*, Vol. 21, No. 3, 2014, pp. 225–233.

[7] Li, W., G. Q. Fu, M. S. Chu, and M. Y. Zhu. Effect of porosity of Hongge vanadium titanomagnetite-oxidized pellet on its reduction swelling behavior and mechanism with hydrogen-rich gases. *Powder Technology*, Vol. 343, 2019, pp. 194–203.

[8] He, W. C., X. W. Lv, Y. Zhang, and X. Q. Li. Thermodynamic calculations on electric furnace smelting separation of chromium-bearing vanadium titanium magnetite. Springer, Cham, 2018, pp. 167–175.

[9] Zhou, M., T. Jiang, X. Y. Ding, S. H. Ma, G. Wei, and X. X. Xue. Thermodynamic study of direct reduction of high-chromium Vanadium-titanium magnetite (HCVTM) based on phase equilibrium calculation model. *Journal of Thermal Analysis and Calorimetry*, Vol. 111, No. 45, 2007, pp. 16927–16933.

[10] Tang, J., M. S. Chu, C. Feng, Y. T. Tang, and Z. G. Liu. Melting separation behavior and mechanism of high-chromium vanadium–bearing titanomagnetite metallized pellet got from gas-based direct reduction. *ISIJ International*, Vol. 56, No. 2, 2016, pp. 210–219.

[11] Cheng, G. J., J. X. Liu, Z. G. Liu, M. S. Chu, and X. X. Xue. Non-isothermal reduction mechanism and kinetics of high chromium vanadium–titanium magnetite pellets. *Ironmaking & Steelmaking*, Vol. 42, No. 1, 2015, pp. 17–26.

[12] Park, E. and O. Ostrovski. Reduction of titania-ferrous ore by carbon monoxide. *ISIJ International*, Vol. 43, No. 9, 2003, pp. 1316–1325.

[13] Park, E, S. B. Lee, and O. Ostrovski. Reduction of the mixture of titanomagnetite ironsand and hematite iron ore fines by carbon monoxide. *ISIJ International*, Vol. 44, No. 1, 2004, pp. 214–216.

[14] Zhang, Y., J. Tang, M. S. Chu, Y. Liu, S. Y. Chen, and X. X. Xue. Optimization of BF slag for high Cr_2O_3 vanadium–titanium magnetite. *Journal of Iron and Steel Research International*, Vol. 21, No. 2, 2014, pp. 144–150.

[15] Chen, S. Y., X. J. Fu, M. S. Chu, L. X. Zhe, Z. G. Liu, and J. Tang. Carbothermic reduction mechanism of vanadium–titanium magnetite. *Journal of Iron and Steel Research International*, Vol. 23, No. 5, 2016, pp. 409–414.

[16] Cheng, G. J., X. X. Xue, Z. X. Gao, T. Jiang, H. Yang, and P. N. Duan. Effect of Cr_2O_3 on the reduction and smelting mechanism of high-chromium vanadium–titanium magnetite pellets. *ISIJ International*, Vol. 56, No. 11, 2016, pp. 1938–1947.

[17] Cheng, G. J., X. X. Xue, T. Jiang, and P. N. Duan. Effect of TiO_2 on the crushing strength and smelting mechanism of high-chromium vanadium–titanium magnetite pellets. *Metallurgical and Materials Transactions. B,* Process Metallurgy and Materials Processing Science, Vol. 47B, No. 3, 2016, pp. 1713–1726.